The Astrophysical Journal Letters, 933:L43 (9pp), 2022 July 10 https://doi.org/10.3847/2041-8213/ac7d5b

Beginning a Journey Across the Universe: The Discovery of Extragalactic Neutrino Factories

Sara Buson[1], Andrea Tramacere[2], Leonard Pfeiffer[1], Lenz Oswald[1], Raniere de Menezes[1], Alessandra Azzollini[1], and Marco Ajello[3]
[1] Lehrstuhl für Astronomie, Universität Würzburg, Emil-Fischer-St. 31, Würzburg, D-97074, Germany; sara.buson@uni-wuerzburg.com
[2] Department of Astronomy, University of Geneva, Ch. d'Ècogia 16, Versoix, 1290, Switzerland; andrea.tramacere@unige.ch
[3] Department of Physics and Astronomy, Clemson University, Kinard Lab of Physics, Clemson, SC 29634-0978, USA
Received 2022 May 13; revised 2022 June 20; accepted 2022 June 28; published 2022 July 14

Abstract

Neutrinos are the most elusive particles in the universe, capable of traveling nearly unimpeded across it. Despite the vast amount of data collected, a long-standing and unsolved issue is still the association of high-energy neutrinos with the astrophysical sources that originate them. Among the candidate sources of neutrinos, there are blazars, a class of extragalactic sources powered by supermassive black holes that feed highly relativistic jets, pointed toward Earth. Previous studies appear controversial, with several efforts claiming a tentative link between high-energy neutrino events and individual blazars, and others putting into question such relation. In this work, we show that blazars are unambiguously associated with high-energy astrophysical neutrinos at an unprecedented level of confidence, i.e., a chance probability of 6×10^{-7}. Our statistical analysis provides the observational evidence that blazars are astrophysical neutrino factories and hence, extragalactic cosmic-ray accelerators.

Unified Astronomy Thesaurus concepts: Neutrino astronomy (1100); Neutrino telescopes (1105); Blazars (164); Supermassive black holes (1663); Relativistic jets (1390); Cosmic ray astronomy (324)

1. Introduction

Cosmic rays are charged particles of energies up to 10^{20} eV, far higher than the most powerful human-attained particle accelerator, i.e., the Large Hadron Collider (LHC). The nature and origin of these particles arriving from deep outer space remain elusive and represent a foremost challenge for the astroparticle and astrophysics fields. Cosmic rays' birthplaces generate other particles, neutrinos and γ rays among them. Unlike γ rays, astrophysical neutrinos are solely created in processes involving cosmic-ray acceleration, making them unique smoking-gun signatures of a cosmic-ray source (Mészáros 2017). In 2013, the IceCube Collaboration reported the discovery of a diffuse flux of astrophysical neutrinos in the $\gtrsim$100 TeV to 10 PeV energy range (IceCube Collaboration 2013; Aartsen et al. 2016). The origin of this diffuse flux is probably extragalactic but still has to be ascertained.

Among the candidate sources of high-energy neutrinos, there are blazars,[4] a class of extragalactic sources powered by supermassive black holes harbored at the center of their host galaxies (Hillas 1984; Winter 2013; Padovani et al. 2015; Palladino et al. 2019). Blazars efficiently convert the gravitational energy of accreting gas into kinetic energy of highly relativistic jets, pointed toward Earth (Padovani et al. 2017). In 2017, the potential association (Aartsen et al. 2018a, 2018b) of the γ-ray-bright blazar TXS 0506 + 056 with putative neutrino emission (chance probability at the $\gtrsim 10^{-4}$ level) has put forward γ-ray blazars as promising neutrino point sources, hence cosmic-ray accelerators (Padovani et al. 2018; Gao et al. 2019; Oikonomou et al. 2021; Keivani et al. 2018; Murase et al. 2018). Further efforts extensively pursued the search for a link between high-energy neutrinos and blazars leading to a large debate, with claimed associations (chance probability $\gtrsim 10^{-3}$) between blazars and high-energy neutrinos (Padovani et al. 2016; Kadler et al. 2016; Plavin et al. 2021; Hovatta et al. 2021; Abbasi et al. 2021), as well as contrasting findings (Aartsen et al. 2017a; Yuan et al. 2020). Previous studies were hampered by employing a sample of blazars selected according to the objects' electromagnetic properties in a preferential energy band. Besides, most searches rely on the assumptions of a correlation between the γ-ray/neutrino emission (Hooper et al. 2019; Giommi et al. 2020; Oikonomou et al. 2019; Garrappa et al. 2019; Franckowiak et al. 2020), often implying that the majority of the observed γ rays originate from the same emission region as neutrinos. As shown by several theoretical studies (e.g., Murase et al. 2016; Reimer et al. 2019; Aartsen et al. 2017a) and observational constraints (Aartsen et al. 2017a; Yuan et al. 2020), however, a bright GeV γ-ray-emitting blazar can unlikely be at the same time an efficient (cospatial) producer of high-energy neutrinos.

In this work, we overcome the limitations of the previous searches by employing the largest available neutrino data set optimized for searches of point-like sources and a homogeneous clean sample of the blazar population. The paper is organized as follows: Section 2 lays out the working hypothesis, Section 3 presents the neutrino data and Section 4 the blazar sample, Section 5 describes the statistical analysis and results, and Sections 6 and 7 present the discussion and conclusions.

2. Working Hypothesis

Blazar theoretical models predict an emerging neutrino spectrum to be hard in the IceCube energy band, with an emission that follows a power law with index $\lesssim -2$ and peaks

[4] For the definition of blazar adopted here we refer the reader to the fifth Roma-BZCat catalog (Massaro et al. 2015).

at $\gtrsim$1 PeV energies (e.g., Mannheim 1993; Stecker 2013; Dermer et al. 2014; Murase et al. 2014; Petropoulou et al. 2015; Padovani et al. 2015). The bulk of the blazars' neutrino emission should reside at energies $\gtrsim$1 PeV. Besides invoking theoretical models in support of this hypothesis, it is demanded by observational constraints, such as the IceCube collaboration stacking limit on γ-ray blazars (Aartsen et al. 2017a), which already excludes a substantial (<27%) contribution from this population in the $\sim$10 TeV/100 TeV energy range for an emerging neutrino soft spectrum ($\propto E^{-2.5}$). The limit relaxes to 40% and 80% when assuming a hard spectrum, e.g., a power-law spectrum $\propto E^{-2.0}$, compatible with the IceCube diffuse flux measured above $\sim$200 TeV (Aartsen et al. 2016). Similar conclusions are drawn by independent, complementary studies (e.g., Yuan et al. 2020).

Motivated by these primers, one may foresee a correlation between blazars and astrophysical neutrinos, especially those of the highest observable energies ($\gtrsim$100 TeV). The IceCube Observatory is sensitive to different astrophysical neutrino energy ranges in the southern and northern celestial hemispheres. Given its location at the geographic south pole, Earth's opacity hampers the detection of the highest-energy astrophysical neutrinos from the northern hemisphere; for $\gtrsim$100 TeV neutrino energies, the effect starts to be important at $\delta \sim 30°$. Therefore, the data collected for the northern sky are best capable of probing the TeV/sub-PeV range while the southern data are most sensitive to astrophysical neutrino fluxes in the PeV−EeV range (Abbasi et al. 2009, see also next Section 3). Because this work aims to test the hypothesis of blazars as high-energy neutrino emitters, we focus our search on the southern hemisphere first, which provides the most promising discovery ground. A forthcoming publication will address the expansion of this investigation to neutrinos observed at the lower energies ($\lesssim$100 TeV).

3. The Neutrino Data Set

The IceCube collaboration has publicly released an all-sky neutrino map encompassing 7 yr of observations recorded with the IceCube Neutrino Observatory between 2008–2015 (Aartsen et al. 2017b). The event sample used to produce this map includes more than 700,000 individual events and was developed to give optimal performance for the identification of point sources emitting neutrinos at TeV energies and above. To this aim, the individual neutrino events were analyzed using an unbinned likelihood formalism, which takes advantage of the good angular reconstruction and large statistics of the data set (Aartsen et al. 2017b). The all-sky map produced with such analysis encodes the information about the 7 yr time-integrated neutrino emission from steady point-source neutrino emitters.

The IceCube map provides for each direction of the sky at decl. $|\delta| < 85°$ a local probability (p-value), in a grid of $0.^{\circ}1 \times 0.^{\circ}1$ pixels. The local p-value represents the level of clustering in the neutrino data, i.e., a measure of the significance of neutrino events being uniformly distributed. They are not to be confused with the statistical p-values derived from our correlation study presented in the following. In our analysis, we adopt the negative logarithm of the provided local p-value, defined as $L = -\log(p\text{-value})$. The neutrino L values range from 0 to 5.9 and are based on the likelihood of the model assuming an astrophysical source with a power-law spectrum in a given direction of the sky. Our work treats the local L values as an inference of the direction-dependent neutrino emission, i.e., larger values of L imply a higher probability that a genuine astrophysical signal is responsible for the spatial clustering of neutrino events in such direction of the sky.

Similarly to the strategy used by the IceCube collaboration, we divide the neutrino data sets at the horizon in two regions: the northern sky with decl. $85° > \delta \geqslant -5°$ and the southern sky with $-85° < \delta < -5°$. This is motivated by the different energy ranges, background characteristics, and analysis techniques applied to the event data sets (Aartsen et al. 2017b).

Among differences, the northern sky data are based on event samples optimized for the search of point-like sources sensitive to both hard and soft or cutoff signal energy spectrum with power-law spectra $\propto E^{-2}$ and $\propto E^{-2.7}$, respectively, and allow an energy threshold as low as few TeV. For the southern sky data, the final event rate is optimized to yield the best sensitivity and discovery potential for an $\propto E^{-2}$ spectrum, and a lower energy threshold of $\sim$100 TeV was adopted (Aartsen et al. 2017b), optimizing the sensitivity and discovery potential for hard-spectrum neutrino signals in the PeV range. The spectral information for the sky map is not available. Due to the differences in the background characteristics and analysis procedures between the northern and southern neutrino data, these may be considered different data sets as well as they may be sensitive to multiple populations of astrophysical sources dominating at different energy ranges and/or with different spectra. As a matter of fact, the IceCube diffuse neutrino spectrum indicates a spectral break and/or an additional soft-spectrum astrophysical component at lower energies (e.g., Aartsen et al. 2016). Contextually, a soft-spectrum (power-law index = 3.4) cluster of neutrinos has been reported consistent with the Seyfert II galaxy NGC 1068 (Aartsen et al. 2020). Given the substantial differences in the properties and energy ranges of the two data sets, to test the working hypothesis introduced in Section 2 in the following, we focus on the southern hemisphere data set.

4. The Blazar Sample

To search for astrophysical counterparts to the neutrino spots we use the fifth data release of Roma-BZCat catalog (5BZCat; Massaro et al. 2015). Although it does not contain all existing blazars in the universe, it is a thorough compilation of 3561 objects of either confirmed or highly likely blazar nature from the literature where each object has been individually inspected to reduce the possibility of including nonblazar sources in the catalog. It has no preferred selection toward a particular wavelength or survey strategy and offers a homogeneous sample of the blazar population. These are major key differences with respect to previous studies that utilized large samples of blazars selected based on well-defined observational or intrinsic properties (Aartsen et al. 2017a; Giommi et al. 2020; Resconi et al. 2017; Plavin et al. 2021; Hovatta et al. 2021).

Each 5BZCat object has a detection in the radio band and complete spectroscopic information available. The only exception are 92 objects that lack an optical spectrum and are thus listed as a "BL Lac candidate." We exclude the latter to maximize the genuineness of our blazar sample. Besides, due to the deficit of 5BZCat sources near the Galactic plane (given by an observational selection effect where extinction from dust in the Milky Way worsens the sensitivity of observations), we discard from our statistical analysis 5BZCat sources located at

Galactic latitudes $|b| < 10°$. We anticipate that a consistent cut is applied in the neutrino sample (see Section 5.1). Furthermore, we discard objects at $|\delta| > 85°$, because neutrino data are not available for regions close to the poles. Dividing the blazar sample according to $\delta < -5°$, our final southern sky sample hosts 1177 objects.

5. Statistical Analysis Procedure

No population of high-energy neutrino point sources has been identified at high confidence at present, preventing us from making a useful a priori choice for the optimal L parameter that maximizes the astrophysical component in the neutrino data (IceCube Collaboration 2013; Aartsen et al. 2014a, 2015, 2016, 2020; Adrián-Martinez et al. 2016). Similarly, the systematic uncertainties related to the neutrino data set are not provided. Given the limited knowledge to guide the selection of the neutrino data, we compute the degree of the blazar/neutrino correlation as a function of two parameters, i.e., the local probability of a neutrino spot to be astrophysical $L_{\rm min}$ and the association radius $r_{\rm assoc}$. These are a posteriori cuts. The estimate of the final posttrial statistical significance will incorporate the effect of the scan over the data, as explained in the following sections. We note that the blazar catalog incompleteness may have some impact on the estimate of the strength and optimal set of parameters that drive the blazar/neutrino correlation. In particular, it may weaken the measured strength of a true correlation (Pierre Auger Collaboration et al. 2008).

5.1. Neutrino Spot Sample

We identify the most likely location of a putative neutrino source as the pixel map, i.e., spot, with the highest value of L above a given choice of $L_{\rm min}$. We adopt the R.A. (α_{hs}) and decl. (δ_{hs}) of the pixel maps as the fiducial sky positions of the spots. We require the separation between neutrino spots to be an angular distance of at least 1° from each other (similarly to, e.g., Aartsen et al. 2017b, 2019), where 1° is the upper limit of the systematic error reported by the IceCube collaboration (IceCube Collaboration 2013; Aartsen et al. 2014b, 2014). The choice of $L_{\rm min}$ is a trade-off between the expected astrophysical signal and trials. It is reasonable to assume that for a large majority of the sky locations tested with the likelihood fit, the clustering in the neutrino data is driven by nonastrophysical components due to background fluctuations (Aartsen et al. 2017b). Therefore, we limit our analysis to the neutrino spots with the highest L, i.e., those with pretrial local significance $>3.5\sigma$ Gaussian equivalent. From the southern sky map, we select spot subsamples defined by a minimum value of $L_{\rm min}$, with $L_{\rm min}$ ranging in [3.5, 4.0, 4.5]. These subsamples count 55, 21, and 10 spots and provide us with a trade-off between the astrophysical signal and background contamination while at the same time limiting the number of trials. Applying the Galactic plane cut, the final neutrino spot subsamples $L3.5$, $L4.0$, and $L4.5$ contain 44, 19, and 9 spots at $|b| > 10°$, respectively.

The $L_{\rm min} = 4.5$ threshold coincides with a 2σ (pretrial) tension from background expectation and is close to the largest deviation (above background) of $L_{\rm min} = 4.66$ observed in the all-sky hotspot population analysis carried out by the IceCube[5] collaboration (Aartsen et al. 2017b). The excess in the neutrino-clustering data around $L \sim 4$ is present also in the one-year data set and three-year data set analysis (Hooper et al. 2019; Smith et al. 2021) and could indicate a near-threshold point-source astrophysical population.

[5] Note that upon correcting for the large number of trials in the all-sky analysis, the excess is not statistically significant (Aartsen et al. 2017b; Hooper et al. 2019; Smith et al. 2021).

5.2. Positional Cross-correlation Analysis

The positional cross-matching strategy employed in the following has been widely used in cross-correlation studies (Finley & Westerhoff 2004; Pierre Auger Collaboration et al. 2008; Resconi et al. 2017; Plavin et al. 2021; Hovatta et al. 2021). Similarly to previous studies (IceCube Collaboration et al al., 2016; Padovani et al. 2016; Giommi et al. 2020), we keep fixed the IceCube hotspot positions, which are known to be not uniformly distributed. We simulate 10^8 Monte Carlo (MC) catalogs by randomizing the blazar positions, preserving both the total number and the spatial distribution of the blazars, as confirmed by the Kolmogorov–Smirnov (KS) tests applied to the spatial distributions. This approach preserves large-scale patterns present in the blazar sample, at the same time allowing us to have a representative set of random cases (Appendix A addresses the robustness and impact of the randomization strategy on the results). To gauge the significance of any excess, the pretrial p-value is computed by inferring for each angular scale scanned the fraction of simulations having more matches than the real data. We retrieve the distance for which this fraction is minimized, the minimum value of this fraction being the pretrial p-value. Finally, the posttrial p-value is calculated as the fraction of simulations that, following a similar analysis, would lead to a smaller pretrial p-value than what was observed in the data.

The optimal association radius between the neutrino spots and blazars is driven by the positional uncertainty of the neutrino data. The median angular resolution of the neutrino data sets ranges from $\lesssim 0.^\circ 4$ to $\lesssim 0.^\circ 7$ for events with an energy proxy of $\sim$100 TeV and improves with increasing energies being below $0.^\circ 6$ at PeV energies (Aartsen et al. 2013, 2017b). Events with higher energies are expected to be most effective in identifying astrophysical signals with hard spectra in the PeV range. Hence, we test a range of association radii $r_{\rm assoc}$ from $0.^\circ 4$ to $0.^\circ 7$.

We perform a grid search approach where we scan the $\{L_{\rm min}, r_{\rm assoc}\}$ space, with $L_{\rm min}$ ranging in [3.5, 4.0, 4.5], and $r_{\rm assoc}$ ranging in [$0.^\circ 4$: $0fdg7$] with a step of $0.^\circ 05$. For each set of ($L^i_{\rm min}$, $r^j_{\rm assoc}$), we match the positions of the 5BZCat objects with the positions of the neutrino spots. The number of real matches constitutes our test statistics, we denote it as $\mathrm{TS}^{L_i,r_j}_{\rm astro}$. Then, we estimate the pretrial p-value, $p^{L_i,r_j}_{\rm pre}$, for the set of parameters following these steps:

1. We generate $N_{\rm MC} = 10^8$ MC catalogs of blazars randomly shifting the sky position of the original 5BZCat sources by a random value between 0° and 10°, applying the same cuts as for the real 5BZCat sample, preserving both the total number and the distribution of our blazar sample. In the randomization, we ensure that the angular distribution of the catalog is preserved by performing KS tests on the distributions of the mock right ascensions and declinations. The mock-catalog distributions obtained in this manner preserve the statistical properties of the original distribution, e.g., their correlation and nonuniformity across the sky.

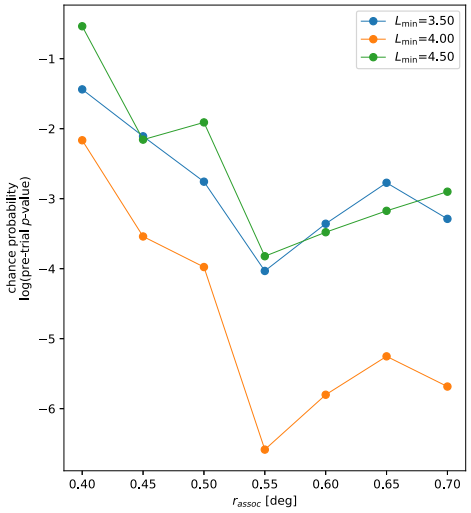

Figure 1. Pretrial p-value for the blazar/neutrino correlation as a function of the association radii $r_{\rm assoc}$, for neutrino data set with $L_{\rm min} = [3.5, 4.0, 4.5]$. The y-axis displays values on a logarithmic scale. The minimum chance probability of 3×10^{-7} is achieved with the set of parameters $L_{\rm min} = 4.0$ and $r_{\rm assoc} = 0.^{\circ}55$. The estimated posttrial chance probability is 6×10^{-7}.

2. We apply the matching procedure between the MC catalogs and neutrino spots. Similarly to what was done for the experimental data, for the mock catalogs, we allow only one mock source to be associated with the same neutrino spot and vice versa. The statistical significance evaluated in this way represents the most conservative approach. However, in reality, a neutrino spot could originate from the cumulative neutrino emission of distinct astrophysical sources located at a distance smaller than the instrumental spatial resolution.
3. The matching procedure yields a distribution of MC test statistics $\mathrm{TS}_k^{L_i,r_j}$, with $k \in [1, N_{\rm MC}]$. We derive the chance probability of obtaining a test statistic value equal to or higher than the one observed for the real data following Davison & Hinkley (1997):

$$p = \frac{M+1}{N+1}, \tag{1}$$

where M is the number of random MC samples with a test statistic equal to or larger than that in the real data, and $N = N_{\rm MC}$ is the total number of random MC samples generated. This is the pretrial p-value, $p_{\rm pre}^{L_i,r_j}$, and defines the probability of a chance coincidence following Equation (1) for the given real set of parameters $(L_{\rm min}^i, r_{\rm assoc}^j)$.

At the end of this procedure, we obtain for each set of $(L_{\rm min}^i, r_{\rm assoc}^j)$ a corresponding pretrial p-value, p^{L_i,r_j}, as shown in Figure 1. The minimum pretrial p-value indicates the optimal set of $(L_{\rm min}^i, r_{\rm assoc}^j)$. In our analysis, this corresponds to a pretrial p-value, $p_{\rm pre}^{\rm best} = 3 \times 10^{-7}$, achieved for $L_{\rm min} = 4.0$ and $r_{\rm assoc} = 0.^{\circ}55$. This minimum pretrial p-value, obtained upon scanning the full space of parameter sets, provides us with the strongest potential correlation signal. As aforementioned, because these optimal values are derived from the data, a statistical penalty has to be evaluated and included in the calculation of the final chance probability, i.e., the posttrial p-value. The latter is evaluated using Equation (1) following the same procedure that we have applied to the real data, as described above, with the difference that in place of $\mathrm{TS}_{\rm astro}^{L_i,r_j}$, we use each of the $\mathrm{TS}_k^{L_i,r_j}$ found from the MC samples. To this aim, we treat each MC sample as a "real observation" and test it against the $N = N_{\rm mock} - 1$ random samples. This provides us with the total occurrences of p-values smaller than or equal to $p_{\rm pre}^{\rm best}$ in the random MC population. This value is used as M in Equation (1), while $N = N_{\rm MC} - 1$. Following this approach, we obtain a posttrial p-value $p_{\rm post}^{\rm best} = 6 \times 10^{-7}$, suggesting that the observed blazar/neutrino correlation is highly unlikely to arise by chance. Table 1 summarizes the outcomes of the statistical analysis.

Table 1
Statistical Significance of Blazar/Neutrino Hotspots Association

Sky Region	5BZCat	Hotspots	Matches	Pretrial p-value	Posttrial p-value
Southern sky ($L \geqslant 4$)	1177	19	10	3×10^{-7}	6×10^{-7}

Note. The chance probability of the correlation is estimated by performing 10^8 MC simulations. The posttrial chance probability incorporates the effect of testing several data sets.

6. PeVatron Blazars Hosted in the Southern Neutrino Sky

Figure 2 displays the all-sky IceCube map in equatorial coordinates where we pinpoint the sky positions of the 5BZCat blazars associated with neutrino hotspots, i.e., the PeVatron blazars. Among the southern neutrino sources associated with a BZCat object, with the exception of 5BZU J1819−6345, all hotspot/blazar matches lie within decl. $-40^{\circ} < \delta < -5^{\circ}$, i.e., close to the celestial horizon. This is the region with the best sensitivity of the IceCube Observatory, i.e., where a hard-spectrum astrophysical signal is more likely expected to emerge (Coenders 2016). We note that despite being the blazar/neutrino association statistically robust, roughly half of the neutrino hotspots have no counterpart in 5BZCat. This may be a consequence of the incompleteness of the catalog (Massaro et al. 2015), as is generally the case for active galactic nucleus (AGN) catalogs. At the same time, it opens the possibility of other populations of neutrino emitters with, e.g., different extragalactic and/or galactic counterparts at high latitudes (Aartsen et al. 2020; Cao et al. 2021a, 2021b). Among the nine unassociated hotspots, the majority have decl. $\delta \gtrsim -40^{\circ}$ and thus are promising genuine astrophysical signals. Our result suggests that what we are observing may be the "tip of the iceberg", i.e., the brightest most efficient neutrino emitters. In fact, our statistical analysis focuses only on the handful of highest-significance hotspots. Due to the limited statistics, the optimal set of parameters identified in this work may be regarded as indicative values for the scales at which the correlation may be relevant. Following this pioneering discovery, more lower-confidence associations, hidden in the neutrino data and/or whose counterparts are not in 5BZCat, may be uncovered by more sophisticated techniques (Abbasi et al. 2021) and more complete astrophysical population surveys.

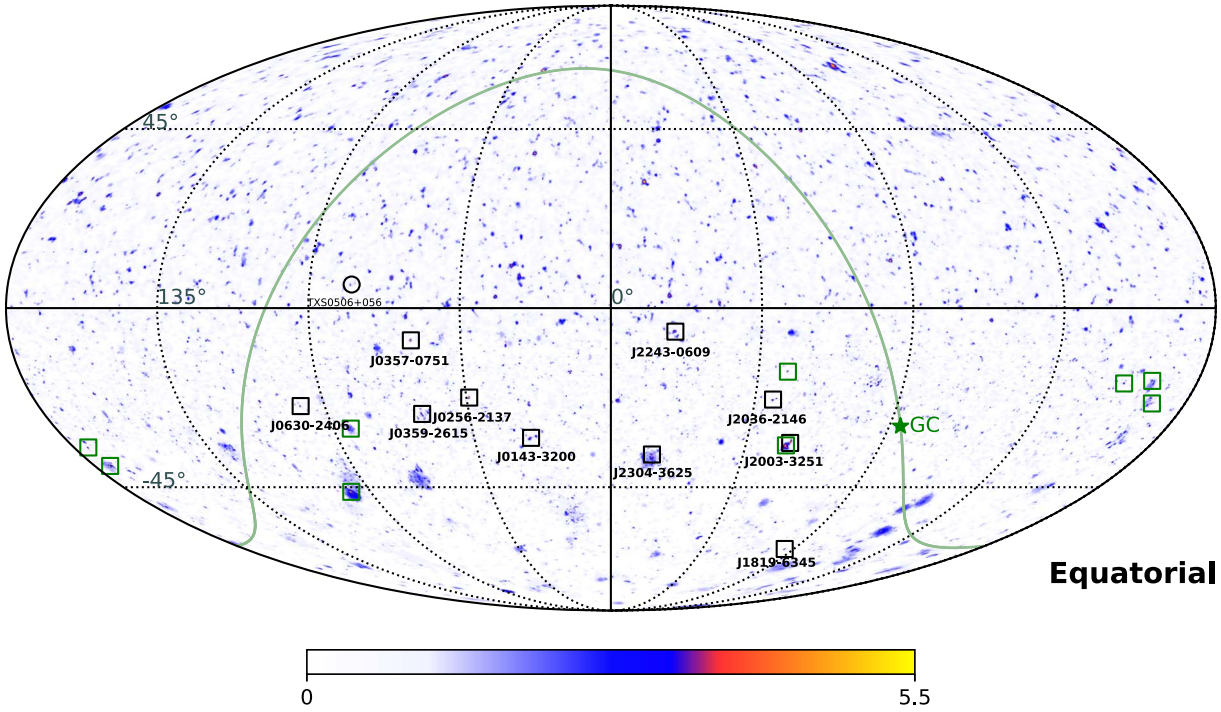

Figure 2. All-sky map in equatorial coordinates (J2000) of the IceCube neutrino local p-value logarithms denoted as L. Locations of PeVatron blazars associated with neutrino hotspots are pointed out by black squares. For visualization clarity, the label of 5BZCat objects is limited to reporting the unique numerical coordinate part. Unassociated hotspots are highlighted by green squares. The location of TXS 0506+056 is shown for reference (green circle). Squares are not to scale and serve the only purpose of highlighting the blazars' locations. The Galactic plane and Galactic center are shown for reference as a green line and star, respectively.

6.1. PeVatron Blazars are Cosmic-Ray Factories

This work proves that at least part of the blazar population originates high-energy neutrinos and, hence, is capable of accelerating cosmic rays. A neutrino with observed energy E must be produced at redshift z with rest-frame energy $E_\nu^{RF} = (1+z)E$. If the neutrinos are produced by acceleration processes within the blazar jet, the relation between the rest-frame and observed energies is $E_\nu^{RF} = (1+z)E/D$, where $D = \frac{1}{\Gamma(1-\beta_\Gamma \cos(\theta))}$, is the beaming factor defined by the bulk Lorentz factor Γ, and θ is the viewing angle of the jet. Typical beaming factors for blazars are of the order of $D \sim 10$ and viewing angles are of the order of $\lesssim$ few degrees. The production of neutrinos of energies E_ν unavoidably requires hadrons to be accelerated to energies $\sim 20 \times E_\nu/Z$, Z being the atomic number (Halzen 2013). For the observed (minimum astrophysical) neutrino energies, i.e., between $\sim$100 TeV to $\sim$10 PeV energies, and assuming the acceleration of protons, the sample of PeVatron blazars diagnoses in situ acceleration of hadrons with energies above the PeV range.

PeVatron blazars are listed in Table 2 along with the redshift information and neutrino hotspot association. The sample of PeVatron blazars presents a fairly large range of redshifts. The finding of a neutrino-emitter association within $\lesssim$280 Mpc (Table 2, z = 0.063), i.e., not much beyond the GZK radius, tantalizes the connection of these newly discovered population of PeVatron blazars to the origin of UHECRs. As not many blazars may live within the GZK horizon, this implies that along with the blazar jet, one may invoke as the production site for the neutrinos additional scenarios such as neutrino emission from AGN-driven winds and/or disk-corona models. The excess of neutrinos in the direction of the misaligned jetted galaxy NGC 1068 reported by the IceCube collaboration (Aartsen et al. 2020) and the detection of hadronic γ rays from ultrafast outflows hosted in AGNs (Ajello et al. 2021) support this hypothesis.

On the opposite side, the objects found at high redshift open to the opportunity of studying the physics of powerful cosmic-ray accelerator sites at cosmological distances beyond the γ-ray cosmic horizon and the GZK horizon. The discovery of PeVatron blazars suggests that, in the cosmic-ray energy spectrum, the extragalactic component may contribute yet below the proton knee energies ($\sim$PeV), putting into question the long-standing assumed postulate that the ankle ($\sim$3 EeV) marks the transition between Galactic and extragalactic cosmic rays.

7. Summary and Conclusions

This analysis finds that 10 out of the 19 IceCube hotspots located in the southern sky likely originated from blazars. We observe a roughly even distribution of neutrino hotspots across the southern sky. This corroborates the hypothesis that the dominant origin of these neutrino sources is blazars, which are isotropically distributed in the sky. The fact that half of the astrophysical-likely hotspots are associated with blazars fosters the idea that these newly discovered PeVatron blazars may be the dominant population of steady neutrino emitters resolved by IceCube at observed energies $E \gtrsim 100$ TeV.

It is important to put the discovery of PeVatron blazars in the context of recent works. Our findings are consistent with previous limits on the contribution by γ-ray blazars to the diffuse high-energy neutrino flux observed by IceCube (Aartsen et al. 2017a, 2021; Yuan et al. 2020), being only a small fraction ($\lesssim$30%) of the neutrino-emitter blazars detected also at GeV γ rays (see also Appendix C). This suggests that in the blazars' engine the neutrino emission is weakly related to

Table 2
List of PeVatron blazars/Neutrino Hotspot Associations Found by This Work

IceCube Hotspots				Blazar Associations		
	α_{hs}[°]	δ_{hs}[°]	L	5BZCat	z	Separation[°]
IC J2243−0540	340.75	−5.68	4.012	5BZB J2243−0609	0.30[c]	0.47
IC J0359−0746	59.85	−7.78	5.565	5BZQ J0357−0751	1.05	0.42
IC J0256−2146	44.12	−21.78	4.873	5BZQ J0256−2137	1.47	0.17
IC J2037−2216	309.38	−22.27	4.664	,5BZQ J2036−2146	2.299	0.51
IC J0630−2353	97.56	−23.89	4.420	5BZB J0630−2406[a,b]	>1.238[d]	0.28
IC J0359−2551	59.94	−25.86	4.356	55BZB J0359−2615[a]	1.47[e]	0.40
IC J0145−3154	26.28	−31.91	4.937	55BZU J0143−3200[a]	0.375	0.42
IC J2001−3314	300.41	−33.24	4.905	5BZQ J2003−3251	3.773	0.53
IC J2304−3614	346.03	−36.24	4.025	5BZQ J2304−3625	0.962	0.24
IC J1818−6315	274.50	−63.26	4.030	5BZU J1819−6345	0.063	0.53
IC J2024−1524	306.12	−15.40	4.454	…	…	…
IC J1256−1739	194.06	−17.66	4.407	…	…	…
IC J1329−1817	202.32	−18.29	4.040	…	…	…
IC J1241−2314	190.37	−23.24	4.288	…	…	…
IC J0538−2934	84.73	−29.57	4.994	…	…	…
IC J2006−3352	301.55	−33.87	4.698	…	…	…
IC J1140−3424	175.17	−34.41	4.082	…	…	…
IC J1138−3915[f]	174.64	−39.26	5.885	…	…	…
IC J0628−4616	97.23	−46.28	4.987	…	…	…

Notes. The columns report the neutrino hotspot equatorial coordinates (J2000) and the L value of the hotspot. The candidate 5BZCat blazar counterpart along with the redshift and the distance between the blazar and hotspot. In the lower part of the table, we report for reference the hotspots without a 5BZCat association.
[a] Blazars listed as γ-ray emitters in 4FGL-DR2 (Ballet et al. 2020).
[b] Blazar listed in 2LAC (Ackermann et al. 2011).
[c] Redshift from Healey et al. (2007).
[d] Redshift from Shaw et al. (2013).
[e] Redshift from Drinkwater et al. (1997).
[f] Hotspot positionally consistent with a neutrino-clustering excess previously identified in the 7 yr data set (Aartsen et al. 2017b) and 3 yr data set (Smith et al. 2021).

the observed γ-ray emission. This implies different production sites for the bulk of the observed neutrinos and GeV γ rays in blazars (Murase et al. 2016; Reimer et al. 2019). The outcomes presented in this paper are in agreement with the conclusions presented by Murase et al. (2016), that γ-ray-weak blazars may harbor efficient cosmic-ray accelerators able to produce ∼PeV neutrinos, motivating to explore physical models with predictions in the X-ray and MeV spectral range.

Our finding indicates a firm indirect detection of extragalactic cosmic-ray factories with in situ acceleration of cosmic rays to PeV energies and, possibly, up to the EeV regime (assuming the acceleration of protons). PeVatron blazars shed a new perspective on the properties of the cosmic-ray spectrum, as well as offer a promising probe to test fundamental particle-physics properties beyond the energy region accessible by LHC. The nondetection of individual $\gtrsim$10 PeV likely astrophysical neutrinos over a decade of IceCube observations (IceCube Collaboration et al. 2021) may imply a physical intrinsic limit for PeVatron blazars, i.e., related to the maximum energy of the parent cosmic rays. Nonetheless, the lack of statistics above tens of PeV could be simply due to the sensitivity of IceCube that at those energies degrades rapidly. In the latter case, PeVatron blazars may accelerate hadrons to much higher energies, fostering the tantalizing prospect that the observed high-energy astrophysical neutrinos and UHECRs could be produced by the same population of cosmologically distributed sources (Waxman 2014; Murase et al. 2012). The forthcoming generation of new neutrino detectors such as IceCube-Gen2 (Aartsen et al. 2021), the Cubic Kilometre Neutrino Telescope (KM3NeT, Adrián-Martínez et al. 2016), the The Pacific Ocean Neutrino Experiment (P-ONE, Agostini et al. 2020), the Radio Neutrino Observatory in Greenland (Aguilar et al. 2021 RNO-G,) and the Giant Radio Array for Neutrino Detection (GRAND, Alvarez-Muniz et al. 2020) project has the potential of shedding light into this.

This work was supported by the European Research Council, ERC Starting grant MessMapp, S.B. Principal Investigator, under contract No. 949555. S.B. and A.T. are grateful for valuable conversation to M. Santander, K. Murase, M. Petropoulou, J. DeLaunay, G. Illuminati, D. Caprioli, D. Bastieri, R. D'Abrusco, M. Giroletti, A. Maselli, F. Massaro, S. I. Stathopoulos, and A. Kouchner. This work has made use of data from the Space Science Data Center (SSDC), a facility of the Italian Space Agency (ASI), and data provided by the IceCube Observatory.

Facility: The IceCube Observatory.

Software: astropy (Astropy Collaboration et al. 2013, 2018), healpy, HEALPix, topcat.

Appendix A
Statistical Analysis Robustness

A.1. Accessing Potential Bias

Given the IceCube location at the south pole, the effective area changes with decl. and energy, therefore, the expected background in the IceCube data depends strongly on the decl.. For the 7 yr sky map provided by Aartsen et al. (2017b) the final p-values reported in each sky pixel have been trial-corrected accounting for the chance of background fluctuations

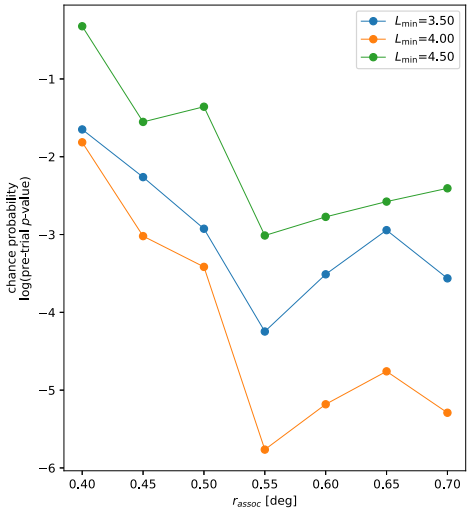

Figure 3. Same as Figure 1 but obtained by randomizing the neutrino spot positions in R.A. (see Appendix A.1). Pretrial p-value for the blazar/neutrino correlation as a function of the association radii $r_{\rm assoc}$ for the neutrino data set with $L_{\rm min} = [3.5,4.0,4.5]$. The y-axis displays values on a logarithmic scale. The minimum chance probability of 1.7×10^{-6} is achieved with the set of parameters $L_{\rm min} = 4.0$ and $r_{\rm assoc} = 0.55°$. The estimated posttrial chance probability is 1.8×10^{-6}.

occurring at any position in the sky. The sky map p-values, that represent the neutrino-clustering probabilities (i.e., L-values), obtained in such a manner are thus decl. independent (Aartsen et al. 2017b).

As an a posteriori, further robustness test, we repeated the cross-correlation analysis by keeping the blazar sky distribution fixed and randomizing the IceCube neutrino spots. This was done by randomizing the R.A. of the neutrino spots while keeping their decl. fixed, thus accounting for the potential, unaccounted for decl. dependence in the IceCube acceptance, and repeating the steps of the statistical analysis described in the main text. This procedure yields a minimum pretrial p-value of 1.7×10^{-6}, which is achieved for $L_{\rm min} = 4.0$ and $r_{\rm assoc} = 0.55°$, and a posttrial p-value of 1.8×10^{-6} (see Figure 3). A slighter higher posttrial p-value with respect to the one in Table 1 is expected because in these experiments, the randomization is applied only to the R.A..

A.2. Null Hypothesis Statistical Properties

The statistical positional correlation analysis presented in Section 5 performs 10^8 simulations, implemented as $10^2 \times 10^6$ mocks for computational reasons, where we randomly shift the sky position of the original 5BZCat sources by a random value between 0° and 10°. In the randomization, we ensure that the angular distribution of the catalog is preserved by performing KS tests on the distributions of the R.A. and declinations between the real (5BZCat) and mock catalog. For each simulation of the 10^6 run, we record the corresponding KS p-values. Once the full run is completed, we record the minimum KS p-value among them for both the RA and decl. distributions. This process is repeated 10^2 times, in order to obtain 10^8 simulations. The total number of 10^8 simulations to be performed is imposed by the requirement of observing an equal number or more of matches as observed in the real data ($\geqslant$10 matches) in at least one mock simulation (frequentist approach).

In the 5BZCat randomization procedure, the majority (95% quantile) of the minimum KS p-values obtained for the mocks versus real data distributions have minimum KS p-values larger than $\sim$0.1 and $\sim$0.07 for RA and decl., respectively. The lowest minimum p-value recorded is 0.02. Such KS p-values ensure that the mock sky distributions are compatible with the original distribution, i.e., the mock distributions obtained in this manner preserve the statistical properties of the null hypothesis. The same validation is performed on the a posteriori neutrino hotspot randomization (see Appendix A.1), yielding consisting results.

Appendix B
Comparison to All-sky Neutrino Hotspot Population Searches

The nonobservation of individual neutrino sources, i.e., hotspots with $L \gg 6$, in the previous searches is not in conflict with our results. Neutrino hotspots represent the level of spatial clustering in the neutrino data at a given sky location. Therefore, none of the neutrino hotspots, and consequently the blazars associated, may necessarily be detected at high confidence by IceCube. Besides, the all-sky scan performed by, e.g., Aartsen et al. (2017b) and similar searches (Hooper et al. 2019; Smith et al. 2021) requires the astrophysical signal hypothesis to exceed the highest background fluctuations from many trials in order to be significant. Implying that, although the IceCube all-sky analysis is sensitive to an astrophysical signal from any direction, the source requires a strong flux to be significantly detected individually in the all-sky scan (Coenders 2016). Even if each neutrino source is not individually detected, the statistical cross-correlation technique presented here has the capability of pinpointing a correlation between subthreshold genuine astrophysical neutrino emitters and astrophysical sources. In principle, more than one astrophysical object may contribute to enhancing the neutrino-clustering local p-value for a spot. Accordingly, our finding claims neither that all 5BZCat sources are neutrino emitters nor that the PeVatron blazars emit neutrinos at the same level. It rather unravels a subpopulation of blazars that may host more efficient hadronic accelerators at $\sim$PeV energies.

Appendix C
Comparison to Previous Works on Gamma-Ray-selected Blazars

Previous works applied a neutrino-stacking analysis to infer limits on the cumulative neutrino emission from γ-ray blazars listed in the second Fermi-LAT AGN Catalog (2LAC; Ackermann et al. 2011). Results from Aartsen et al. (2017a) showed that 2LAC blazars contribute $\lesssim$27% to the diffuse neutrino flux between 10 TeV and 2 PeV when assuming a power-law spectrum with a spectral index of -2.5. The constraint weakens (Aartsen et al. 2018b) to about 40%$-$80% of the total observed neutrino flux assuming a spectral index of -2, as it is observed for the astrophysical diffuse flux at the higher energies ($\gtrsim$200 TeV, Aartsen et al. 2016). Among the 10 neutrino-blazar associations found by our work and listed in Table 2, only 1 was reported as a γ-ray emitter in the 2LAC and hence included in the stacking analysis. Thus, our finding is consistent with previous neutrino-stacking limits reported by the IceCube collaboration.

We note that three of the associated blazars have a counterpart at γ rays in the fourth Fermi-LAT Catalog (4FGL-DR2; Ballet et al. 2020), suggesting that in the future, more neutrino-emitter blazars may be detectable also at γ rays. The newly discovered PeVatron blazars may represent an emerging population of weak γ-ray emitters, potentially detectable with larger accumulation of statistics with the Fermi-LAT and/or the enhanced sensitivity of Cherenkov telescopes. However, the lack of γ-ray counterparts for most of the associations in Table 2 supports the idea that the γ-ray brightness of a blazar in the Fermi-LAT energy band (GeV energies) may be not necessarily correlated with the neutrino brightness, in agreement with Murase et al. (2016).

Appendix D
Comparison to Previous Neutrino/Blazars Correlation Studies

Conflicting results exist regarding a possible link between the radio brightness of blazars and putative neutrino emission (Plavin et al. 2021; Hovatta et al. 2021; Zhou et al. 2021). The 5BZCat catalog includes archival information about the integrated-radio flux in the bands 1.4 GHz and 5 GHz for each object. We do not observe any noteworthy difference in the integrated-radio flux in the bands 1.4 GHz and 5 GHz for the neutrino-emitter blazars found by our work and the other 5BZCat sources. This is consistent with the findings of Hovatta et al. (2021) and Zhou et al. (2021), which report a low level of correlation (chance probability $\gtrsim$0.6%) between AGNs selected at these frequencies and IceCube neutrinos. For reference, the radio-selected sample from Plavin et al. (2021) has 715 objects included in 5BZCat. Because that study (Plavin et al. 2021) focuses on the northern hemisphere only, no direct comparison with our work can be drawn.

Another study by Luo & Zhang (2020) reports no evidence for a correlation between the 5BZCat sources and a sample of 45 IceCube high-energy neutrino events. The main difference with the work presented here is the neutrino data set. The former study uses a small number (45) of individual neutrino high-energy events. We make use of an all-sky neutrino map that exploits the large statistics of neutrino events accumulated over 7 yr. The all-sky map is built with a refined likelihood analysis where the neutrino data are optimized for searches of point-like neutrino sources with a hard power-law spectrum.

A search for a correlation between 5BZCat objects and IceCube neutrinos by Hooper et al. (2019) led to inconclusive results. The main difference is that Hooper et al. (2019) utilize only one year of neutrino data (the 86-string data), while in our work we employ a larger data set collected over a longer period of time.

Appendix E
TXS 0506+056: a Promising PeVatron Blazar

Based on our work one may predict that the IceCube observatory will reach the sensitivity to detect individual astrophysical point sources at high confidence in the near future. This behavior is yet observed at the location of TXS 0506+056, associated with the 5BZCat object 5BZB J0509 + 0541, and has been claimed to be a neutrino-emitter blazar (Aartsen et al. 2018a). In the 7 yr IceCube data utilized by this work, it appears in spatial agreement with a neutrino spot of $L = 2.2$. Because it is located in the northern hemisphere, this blazar is not included in our statistical analysis. However, we note that in the analysis of 10 (8) yr of IceCube observations (Aartsen et al. 2020, 2019), i.e., 3 (2) additional years compared to the all-sky map used by us, the value of L in coincidence with TXS 0506+056 progressively increases to 3.72 (2.65), as expected for a truly astrophysical signal that keeps steadily increasing when deepening the observational sensitivity and acquiring more exposure. Besides, Aartsen et al. (2020) report that the cumulative 10 yr signal at the location of TXS 0506+056 is best fitted by a hard power-law ($\propto E^{-2.1}$) neutrino spectrum, which is consistent with predictions of blazar hadronic models. This corroborates the hypothesis that this blazar may be a genuine astrophysical neutrino source. It would be interesting applying our analysis to the IceCube 10 yr all-sky likelihood map, which has not been released publicly at the time of the writing.

ORCID iDs

Sara Buson https://orcid.org/0000-0002-3308-324X
Andrea Tramacere https://orcid.org/0000-0002-8186-3793
Leonard Pfeiffer https://orcid.org/0000-0003-2497-6836
Lenz Oswald https://orcid.org/0000-0003-4519-4796
Raniere de Menezes https://orcid.org/0000-0001-5489-4925
Alessandra Azzollini https://orcid.org/0000-0002-2515-1353
Marco Ajello https://orcid.org/0000-0002-6584-1703

References

Aartsen, M., Ackermann, M., Adams, J., et al. 2014, ApJ, 796, 109
Aartsen, M., Ackermann, M., Adams, J., et al. 2018a, Sci, 361, 6398
Aartsen, M., Ackermann, M., Adams, J., et al. 2018b, Sci, 361, 147
Aartsen, M. G., Abraham, K., Ackermann, M., et al. 2017a, ApJ, 835, 45
Aartsen, M. G., Abbasi, R., Abdou, Y., et al. 2013, ApJ, 779, 132
Aartsen, M. G., Ackermann, M., Adams, J., et al. 2014a, PhRvL, 113, 101101
Aartsen, M. G., Abbasi, R., Abdou, Y., et al. 2014b, PhRvD, 89, 102004
Aartsen, M. G., Abraham, K., Ackermann, M., et al. 2015, PhRvL, 115, 081102
Aartsen, M. G., Abraham, K., Ackermann, M., et al. 2016, ApJ, 833, 3
Aartsen, M. G., Abraham, K., Ackermann, M., et al. 2017b, ApJ, 835, 151
Aartsen, M. G., Ackermann, M., Adams, J., et al. 2019, EPJC, 79, 3/234
Aartsen, M. G., Ackermann, M., Adams, J., et al. 2020, PhRvL, 124, 051103
Aartsen, M. G., Abbasi, R., Ackermann, M., et al. 2021, JPhG, 48, 060501
Abbasi, R., Abdou, Y., Abu-Zayyad, T., et al. 2009, PhRvL, 103, 221102
Abbasi, R., Ackermann, M., Adams, J., et al. 2021, arXiv:2111.10169
Ackermann, M., Ajello, M., Allafort, A., et al. 2011, ApJ, 743, 171
Adrián-Martinez, S., Albert, A., André, M., et al. 2016, ApJ, 823, 65
Adrián-Martínez, S., Ageron, M., Aharonian, F., et al. 2016, JPhG, 43, 084001
Agostini, M., Böhmer, M., Bosma, J., et al. 2020, NatAs, 4, 913
Aguilar, J. A., Allison, P., Beatty, J. J., et al. 2021, JInst, 16, P0302
Ajello, M., Baldini, L., Ballet, J., et al. 2021, ApJ, 921, 144
Alvarez-Muniz, J., Alves Batista, R., Balagopal, V., et al. 2020, SCPMA, 63, 219501
Astropy Collaboration, Robitaille, T. P., Tollerud, E. J., et al. 2013, A&A, 558, A33
Astropy Collaboration, Price-Whelan, A. M., Sipőcz, B. M., et al. 2018, AJ, 156, 123
Ballet, J., Burnett, T., Digel, S., & Lott, B. 2020, arXiv:2005.11208
Cao, Z., Aharonian, F. A., An, Q., et al. 2021a, Natur, 594, 33
Cao, Z., Aharonian, F., An, Q., et al. 2021b, ApJL, 919, L22
Coenders, S. 2016, PhD thesis, Technical Univ. of Munich, Germany
Davison, A., & Hinkley, D. C. 1997, Bootstrap Methods and their Application Cambridge: Cambridge Series in Statistical and Probabilistic Mathematics (Cambridge: Cambridge Univ. Press)
Dermer, C. D., Murase, K., & Inoue, Y. 2014, JHEAp, 3, 29
Drinkwater, M. J., Webster, R. L., Francis, P. J., et al. 1997, MNRAS, 284, 85
Finley, C. B., & Westerhoff, S. 2004, APh, 21, 359
Franckowiak, A., Garrappa, S., Paliya, V., et al. 2020, ApJ, 893, 162

Gao, S., Fedynitch, A., Winter, W., & Pohl, M. 2019, NatAs, 3, 88
Garrappa, S., Buson, S., Franckowiak, A., et al. 2019, ApJ, 880, 103
Giommi, P., Glauch, T., Padovani, P., et al. 2020, MNRAS, 497, 865
Halzen, F. 2013, APh, 43, 155
Healey, S. E., Romani, R. W., Taylor, G. B., et al. 2007, ApJS, 171, 61
Hillas, A. M. 1984, ARA&A, 22, 425
Hooper, D., Linden, T., & Vieregg, A. 2019, JCAP, 2019, 012
Hovatta, T., Lindfors, E., Kiehlmann, S., et al. 2021, A&A, 650, A83
IceCube Collaboration 2013, Sci, 342, 1242856
IceCube Collaboration, Pierre Auger Collaboration & Telescope Array Collaboration 2016, JCAP, 2016, 037
IceCube Collaboration, Aartsen, M. G., Abbasi, R., et al. 2021, Natur, 591, 220
Kadler, M., Krauß, F., Mannheim, K., et al. 2016, NatPh, 12, 807
Keivani, A., Murase, K., Petropoulou, M., et al. 2018, ApJ, 864, 84
Luo, J.-W., & Zhang, B. 2020, PhRvD, 101, 103015
Mannheim, K. 1993, A&A, 269, 67
Massaro, E., Maselli, A., Leto, C., et al. 2015, Ap&SS, 357, 1
Mészáros, P. 2017, ARNPS, 67, 45
Murase, K., Dermer, C. D., Takami, H., & Migliori, G. 2012, ApJ, 749, 63
Murase, K., Guetta, D., & Ahlers, M. 2016, PhRvL, 116, 071101
Murase, K., Inoue, Y., & Dermer, C. D. 2014, PhRvD, 90, 023007
Murase, K., Oikonomou, F., & Petropoulou, M. 2018, ApJ, 865, 124
Oikonomou, F., Murase, K., Padovani, P., Resconi, E., & Mészáros, P. 2019, MNRAS, 489, 4347
Oikonomou, F., Petropoulou, M., Murase, K., et al. 2021, JCAP, 2021, 082
Padovani, P., Giommi, P., Resconi, E., et al. 2018, MNRAS, 480, 192
Padovani, P., Petropoulou, M., Giommi, P., & Resconi, E. 2015, MNRAS, 452, 1877
Padovani, P., Resconi, E., Giommi, P., Arsioli, B., & Chang, Y. L. 2016, MNRAS, 457, 3582
Padovani, P., Alexander, D. M., Assef, R. J., et al. 2017, A&ARv, 25, 2
Palladino, A., Rodrigues, X., Gao, S., & Winter, W. 2019, ApJ, 871, 41
Petropoulou, M., Dimitrakoudis, S., Padovani, P., Mastichiadis, A., & Resconi, E. 2015, MNRAS, 448, 2412
Pierre Auger Collaboration, Abraham, J., Abreu, P., et al. 2008, APh, 29, 188
Plavin, A. V., Kovalev, Y. Y., Kovalev, Y. A., & Troitsky, S. V. 2021, ApJ, 908, 157
Reimer, A., Böttcher, M., & Buson, S. 2019, ApJ, 881, 46
Resconi, E., Coenders, S., Padovani, P., Giommi, P., & Caccianiga, L. 2017, MNRAS, 468, 597
Shaw, M. S., Romani, R. W., Cotter, G., et al. 2013, ApJ, 764, 135
Smith, D., Hooper, D., & Vieregg, A. 2021, JCAP, 2021, 031
Stecker, F. W. 2013, PhRvD, 88, 047301
Waxman, E. 2014, PhyOJ, 7, 88
Winter, W. 2013, PhRvD, 88, 083007
Yuan, C., Murase, K., & Mészáros, P. 2020, ApJ, 890, 25
Zhou, B., Kamionkowski, M., & Liang, Y.-f. 2021, PhRvD, 103, 123018